

Article

# Hybrid Beamforming for Multi-User Millimeter-Wave Heterogeneous Networks

Zhannan Li  and Tao Chen \*

College of Information and Communication Engineering, Harbin Engineering University, Harbin 150001, China  
\* Correspondence: chentao@hrbeu.edu.cn

**Abstract:** Millimeter-wave (mmWave) communications are a critical technique with next-generation network characteristics such as ultra-dense small cells can meet the skyrocketing demand for mobile data. Hybrid precoding, which combines analog and digital processing to provide both spatial diversity gains and beamforming, is commonly studied for mmWave communications to lower the power and cost consumption of radio frequency (RF) networks. However, the combination of ultra-dense small cells and ever-increasing data traffic results in massive interference. In this paper, we propose a minimum mean square error (MMSE)-based hybrid beamforming strategy for downlink mmWave MIMO two-tier heterogeneous networks (HetNets). The analog beamforming is generalized by an orthogonal matching pursuit technique. The analog beamforming problem is formulated as a sparse signal recovery problem. An MMSE-based digital beamforming algorithm is proposed to minimize the sum MSE of the user-intended data streams so that the inter- and intra-tier interferences are mitigated iteratively. The simulation results demonstrate the advantageous performance of the proposed hybrid beamforming schemes under different cellular cooperation and data transmission scenarios when hardware constraints are taken into account.

**Keywords:** millimeter wave; hybrid beamforming; hetnets



**Citation:** Li, Z.; Chen, T. Hybrid Beamforming for Multi-User Millimeter-Wave Heterogeneous Networks. *Electronics* **2022**, *11*, 4221. <https://doi.org/10.3390/electronics11244221>

Academic Editors: Adão Silva and J.-C. Chiao

Received: 31 October 2022  
Accepted: 15 December 2022  
Published: 18 December 2022

**Publisher's Note:** MDPI stays neutral with regard to jurisdictional claims in published maps and institutional affiliations.



**Copyright:** © 2022 by the authors. Licensee MDPI, Basel, Switzerland. This article is an open access article distributed under the terms and conditions of the Creative Commons Attribution (CC BY) license (<https://creativecommons.org/licenses/by/4.0/>).

## 1. Introduction

Next-generation wireless networks require various wireless technologies, comprehensive coverage, and a rich spectrum of resources to meet the demand for seamless coverage and increased data rates. The mmWave frequency band ranges from 30 GHz to 300 GHz. As a critical candidate technology for 5G wireless communication, it can provide huge bandwidth. Due to the small wavelengths of mmWave, a large number of antenna elements can be packaged into a small physical area [1–5]. HetNets consist of macrocells and low-power overlaid nodes, which have become another key technology capable of offering better coverage and improving the capacity of wireless networks [6,7].

To increase coverage, large antenna arrays are equipped to transmit and receive gain through digital and analog beamforming. Due to the high costs and complexities of specific mmWave mixed-signal components, a fully digital architecture with a dedicated radio frequency (RF) chain for each antenna is challenging to implement. The analog beamforming is achieved by an analog phase shifter, which adjusts the relative phase by controlling the transmit beam direction digitally. The adaptive gain control units and quantization errors in the analog phase shifter lead to a degradation in performance so analog beamforming is not inappropriate for mmWave systems. Hybrid analog/digital beamforming is a desirable option, as hybrid beamforming has lower complexity and consumption than digital beamforming and better system performance than analog beamforming [8,9].

Hybrid beamforming designs for multi-users in mmWave systems were investigated in [10–15]. These works took advantage of the limited scattering properties of the mmWave channel and a few RF chains to power massive antenna arrays, which compromised performance and consumption while achieving almost optimal performance. The work

in [10] proposed two-stage hybrid beamforming with limited feedback for multi-user millimeter-wave systems. The hybrid beamforming design was inspired by the power consumption of signal hardware and the complete radio frequency. A deep-learning massive MIMO mmWave network for a hybrid beamforming strategy was proposed in [11]. A hybrid precoder was selected based on a deep neural network through training. In [12], a low-complexity two-stage hybrid beamforming strategy was proposed for a downlink multi-RF-chain multi-user mmWave network. The out-of-band spatial information was used to minimize the MMSE in transmitting data streams. The works in [13–15] investigated hybrid beamforming in mmWave networks by jointly considering large antenna arrays, RF hardware constraints, and the limited scattering nature of mmWave channels. The work in [13] proposed an iterative strategy by exploiting the duality of the downlink and uplink channels for the joint hybrid beamforming design. The work in [14] proposed a hybrid iterative block structure and analog and digital beamforming were jointly optimized for multi-user massive MIMO mmWave networks.

HetNets based on mmWave and massive multiple-input multiple-output (MIMO) techniques have emerged as a possible alternative for improving the capacity and coverage of next-generation networks. Large antenna arrays are necessary for mmWave systems to achieve a sufficient array gain and a usable connection margin. In a HetNet, the higher-powered macrocells cover a large area, whereas the lower-powered small cells fill in the coverage gaps. There are two types of interference in HetNet: inter- and intra-tier interferences. Picocells interfering with each other is an example of intra-tier interference, which is when there is interference among cells in the same tier. Interference among cells in different tiers, such as when macrocells and picocells interfere with one another, is referred to as inter-tier interference. Optimizing hybrid beamforming in mmWave HetNet systems to improve performance was studied in [16,17]. The work in [16] proposed hybrid beamforming techniques to mitigate interference for ultra-dense massive MIMO mmWave HetNets. In [17], hybrid beamforming designs were investigated in massive MIMO relaying mmWave HetNets. Inter-user interference and cross-tier interference were efficiently addressed. The works in [18,19] provided analytical frameworks for analyzing the coverage of mmWave HetNets. The work in [18] analyzed coverage for energy-harvesting mmWave systems by considering power transfer and downlink simultaneous wireless information. The work in [19] provided an analytical framework by analyzing downlink mmWave HetNets, which consisted of randomly located base stations (BSs) and  $K$  tiers. There are many techniques for reducing interference, including interference alignment (IA) and CoMP. The works in [20,21] utilized IA approaches to address interference in HetNets. The works in [20] proposed a cognitive IA-based scheme to eliminate cross-tier interference in macrocells and mitigate co-tier interference at the same time. The works in [21] analyzed IA methods based on various levels of inter-system information sharing. However, it is pretty challenging to execute interference cancellation in the same manner for different HetNet designs since some small cells clutter in various small locations for various HetNets. Because of a lack of freedom to adapt to different system configurations, IA-type schemes are inflexible.

In this paper, an MMSE-based hybrid beamforming scheme is proposed for downlink mmWave MIMO two-tier HetNets. First, the sum-rate maximization problem is formulated to minimize the MSE between hybrid and digital beamforming solutions with numerous measurement vectors. Analog beamforming is generalized by utilizing an orthogonal matching pursuit technique, wherein the beam-steering vectors are considered to be linearly combined in the RF precoding. Then, the proposed digital beamforming is implemented by iteratively minimizing the sum MSE of the user-intended data streams to manage inter- and intra-tier interferences. Digital beamforming solutions are optimized by utilizing effective channels based on the sequence of analog beamforming weights. The simulation results show the superior performance of the proposed hybrid beamforming scheme under different cellular cooperation and data transmission scenarios.

This paper is organized as follows. In Section 2, the system model for the mmWave HetNet is outlined. In Section 3, we introduce the channel model. In Section 4, we show the problem formulation. Section 5 presents the proposed novel hybrid algorithms based on OMP and MMSE criteria for mmWave HetNets. In Section 6, the simulation results are shown. Section 7 presents the conclusion.

### 2. System Model

As illustrated in Figure 1, we consider a two-tier downlink mmWave HetNet, which comprises a macrocell and multiple picocells. The picocells are divided into two different sub-systems according to the intra-tier interference. Plotted with solid lines, sub-system 1 contains a dense concentration of picocells, making it vulnerable to significant intra-tier interference from other picocells. In sub-system 2, each picocell (shown with dotted lines) is not adjacent to another and will not experience substantial intra-tier interference. Since picocells are within the macrocell coverage area, all pico UEs (pUEs) will suffer inter-tier interference from the macrocell base station (MBS). Both the macrocell and picocells use the mmWave hybrid architecture with ULA deployment. We assume that OFDM signaling with a  $K$ -subcarrier is implemented in this mmWave HetNet system. The BSs and UEs use the same mmWave frequency band in the two-tier HetNet. The  $i$ th base station (BS) is equipped with  $N_i$  antennas and  $N_i^{RF}$  RF chains, which are used to enable multi-stream transmission. The  $i$ th BS communicates with  $L_m$  UEs. The  $m$ th UE in the  $i$ th BS has  $N_u$  antennas and  $N_u^{RF}$  chains.  $\mathbf{s}_i[k] = [\mathbf{s}_{id_1}^T[k], \mathbf{s}_{id_2}^T[k], \dots, \mathbf{s}_{id_{L_m}}^T[k]]^T \in \mathbb{C}^{L_m N_s}$  is denoted as the signal matrix in the  $i$ th cell, where  $i \in \{1, \dots, L\}$ ,  $N_s$  is the number of data streams,  $L$  is the number of cells, and  $i = 1$  represents the macrocell. Here, we examine two communication scenarios: with cooperation and without cooperation among all BSs. In the with-cooperation scenario, the received signal at the  $m$ th UE in the  $i$ th BS is expressed as

$$\mathbf{x}_{mi}[k] = \sum_{1 \leq i \leq L} \mathbf{h}_{mi}[k] \sum_{1 \leq j \leq L} \mathbf{F}_i \mathbf{w}_{ij}[k] \mathbf{s}_j[k] + \mathbf{n}_i[k], \tag{1}$$

and in the without-cooperation scenario, the transmit signal is denoted as

$$\mathbf{x}_{mi}[k] = \mathbf{h}_{mi}[k] \mathbf{F}_i \mathbf{w}_{ii}[k] \mathbf{s}_i[k] + \sum_{j \neq i, 1 \leq j \leq L} \mathbf{h}_{mj}[k] \mathbf{F}_j \mathbf{w}_{jj}[k] \mathbf{s}_j[k] + \mathbf{n}_i[k]. \tag{2}$$

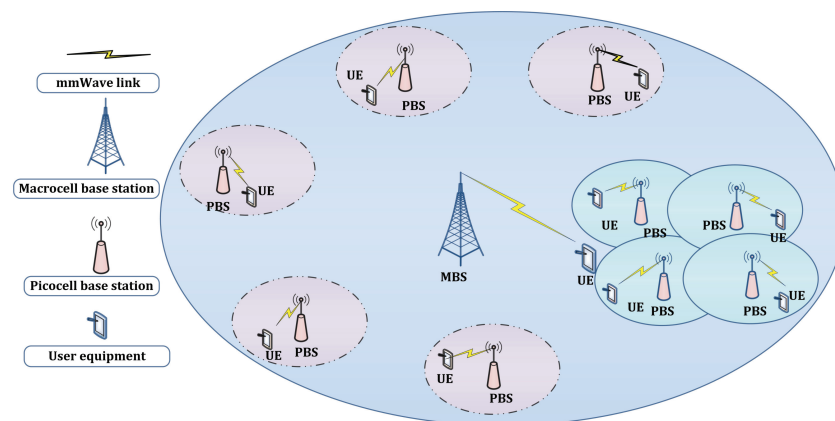


Figure 1. An mmWave HetNet model.

As shown in Figure 2, the hybrid architecture enables the BS to apply a digital precoder  $\mathbf{w}_{ij}[k] = [\mathbf{w}_{id_1}[k], \mathbf{w}_{id_2}[k], \dots, \mathbf{w}_{id_{L_m}}[k]] \in \mathbb{C}^{N_i^{RF} \times L_m N_s}$  of the  $i$ th BS for the signal  $\mathbf{s}_j[k]$ , followed by an analog precoder  $\mathbf{F}_i \in \mathbb{C}^{N_i \times N_i^{RF}}$ , which is employed by analog phase shifters and has the constraints with  $(\mathbf{F}_i \mathbf{F}_i)_{l,l} = \frac{1}{N_i}$ .  $\mathbf{h}_{mi}[k]$  is denoted as the mmWave channel matrix from  $i$ th BS to the  $m$ th UE.  $\mathbf{n}_i[k] \sim \mathcal{CN}(0, \sigma_i^2 \mathbf{I}_{N_i})$  is a zero-mean additive white Gaus-

sian noise matrix and  $\Phi_{ni}[k]$  is its covariance matrix. Both (1) and (2) can be conveniently expressed in the following unified form:

$$\mathbf{x}_{mi}[k] = \mathbf{H}_{mi}[k] \mathbf{F}_i \mathbf{W}_{mi}[k] \mathbf{s}_i[k] + \sum_{j \neq i, 1 \leq j \leq L} \mathbf{H}_{mi}[k] \mathbf{F}_j \mathbf{W}_{mj}[k] \mathbf{s}_j[k] + \mathbf{n}_i[k], \quad (3)$$

where the channel  $\mathbf{H}_{mi}[k] = [\mathbf{h}_{m1}[k] \mathbf{h}_{m2}[k] \cdots \mathbf{h}_{mL}[k]]$ . In the with-cooperation case, the digital precoder matrix  $\mathbf{W}_{mj}[k] = [\mathbf{w}_{1j}^*[k] \mathbf{w}_{2j}^*[k] \cdots \mathbf{w}_{Lj}^*[k]]^*$ . In the without-cooperation case,  $\mathbf{W}_{mj}[k] = [\mathbf{0}_{1j}^*[k] \cdots \mathbf{w}_{ij}^*[k] \cdots \mathbf{0}_{Lj}^*[k]]^*$ . At the  $i$ th UE side, an analog combiner  $\mathbf{F}_{iu_m} \in \mathbb{C}^{N_u \times N_u^{RF}}$  and a digital combiner  $\mathbf{W}_{iu_m}[k] \in \mathbb{C}^{N_u^{RF} \times N_s}$  are implemented for the received signal processing. Then, the combined signal at the  $m$ th UE in the  $i$ th BS is defined as

$$\mathbf{y}_{mi}[k] = \mathbf{W}_{iu_m}^*[k] \mathbf{F}_{iu_m}^* \mathbf{x}_{mi}[k]. \quad (4)$$

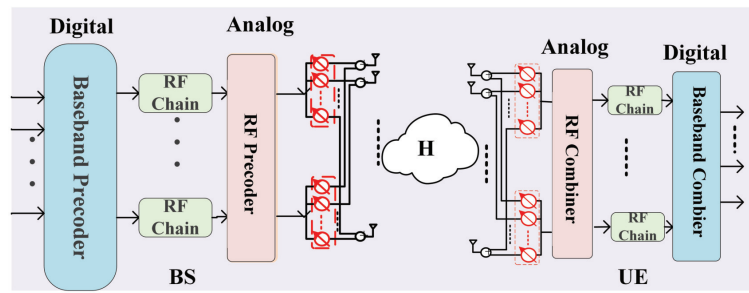


Figure 2. Hybrid analog/digital beamforming architecture.

### 3. Channel Model

This paper adopts a wideband geometric mmWave channel model, which is assumed to contribute  $C$  scattering clusters and  $R_c$  paths per cluster. We assume that both the BSs and UEs have instantaneous and exact knowledge about the channel state information (CSI) of the mmWave channels. The delay- $l$  channel  $\hat{\mathbf{h}}_{mi}[l]$  from the  $i$ th BS to the  $m$ th UE can be written as

$$\hat{\mathbf{h}}_{mi}[l] = \sqrt{\frac{N_i N_u}{\rho}} \sum_{c=1}^C \sum_{r_c=1}^{R_c} \alpha_{r_c} \varrho(l T_s - \tau_c - \tau_{r_c}) \times \mathbf{a}_u(\theta_c + \vartheta_{r_c}) \mathbf{a}_{p_i}^*(\phi_c + \varphi_{r_c}), \quad (5)$$

where  $\tau_c$  and  $\tau_{r_c}$  denote the mean time delay for each cluster and each path, respectively.  $\{\theta_c, \phi_c\}$  is the mean physical AoA/AoD for each cluster.  $\{\vartheta_{r_c}, \varphi_{r_c}\}$  denotes the relative AoA/AoD shift for each path in each cluster.  $T_s$  is the signaling interval,  $\varrho(t)$  is the pulse shaping filter, and  $\rho$  is the large-scale path loss.  $\mathbf{a}_u$  and  $\mathbf{a}_{p_i}$  denote the antenna array response vectors of the UEs and BSs, respectively. The antenna array response vector of the  $i$ th BS can be formulated as

$$\mathbf{a}_{p_i}(\theta) = \frac{1}{\sqrt{N_i}} [1, e^{j \frac{2\pi}{\lambda} d \sin(\theta)}, \dots, e^{j(N_i-1) \frac{2\pi}{\lambda} d \sin(\theta)}]^T, \quad (6)$$

where  $d$  denotes the inter-element spacing and  $\lambda$  is the wavelength. The delay- $l$  channel at the  $k$ th subcarrier  $\mathbf{h}_{ei}[k]$  can be expressed as

$$\mathbf{h}_{mi}[k] = \sum_{l=0}^{D-1} \hat{\mathbf{h}}_{mi}[l] e^{-j \frac{2\pi k}{K} l}, \quad (7)$$

where  $D$  is the number of taps.

#### 4. Problem Formulation

To maximize spectral efficiency, we seek to design the hybrid precoders and combiners ( $\mathbf{W}_{mi}[k], \mathbf{F}_i, \mathbf{W}_{iu_m}[k], \mathbf{F}_{iu_m}$ ) of the BSs and UEs. The sum rate  $\sum_{i=1}^L \sum_{m=1}^{L_m} R_{mi}$  acting as the performance metrics can be expressed as

$$R_{mi} = \frac{1}{K} \sum_{k=1}^K \log_2(1 + v_{mi}[k]), \tag{8}$$

where  $v_{mi}[k]$  denotes the SNR and can be written as

$$v_{mi}[k] = \frac{\|\mathbf{W}_{iu_m}^*[k] \mathbf{F}_{iu_m}^* \mathbf{H}_{mi}[k] \mathbf{F}_i \mathbf{W}_{mi}[k]\|_F}{\sum_{j \neq i}^L \|\mathbf{W}_{iu_m}^*[k] \mathbf{F}_{iu_m}^* \mathbf{H}_{mj}[k] \mathbf{F}_j \mathbf{W}_{mj}[k] \mathbf{s}_j[k]\|_F + \sigma_i^2 \|\mathbf{W}_{iu_m}^*[k] \mathbf{F}_{iu_m}^*\|_F}. \tag{9}$$

To obtain the optimal ( $\mathbf{W}_{mi}[k], \mathbf{F}_i, \mathbf{W}_{iu_m}[k], \mathbf{F}_{iu_m}$ ), the maximization problem can be expressed as

$$\begin{aligned} & \arg \max_{\mathbf{W}_{mi}[k], \mathbf{F}_i, \mathbf{W}_{iu_m}[k], \mathbf{F}_{iu_m}} \sum_{i=1}^L \sum_{m=1}^{L_m} R_{mi}[k], \\ & \text{s.t. } \text{tr}(\mathbf{W}_{mi}^*[k] \mathbf{F}_i^* \mathbf{F}_i \mathbf{W}_{mi}[k]) = P_i, \end{aligned} \tag{10}$$

where  $P_i$  denotes the total transmitting power of the  $i$ th cell. Due to the variable's multiplication and constraints in (10), the optimization problem is nonconvex. Moreover, since the analog precoders are constrained to constant modulus, finding the global optimal joint hybrid beamforming solutions is often intractable. In the following section, the designs for hybrid beamforming are mathematically decoupled and the optimization problem is reformulated. Then, in the subsequent section, the novel hybrid beamforming designs for mmWave HetNets are discussed.

#### 5. Hybrid Beamforming for the mmWave HetNet

The non-convex constraints on the hybrid beamforming designs make finding globally optimal solutions unlikely. Therefore, we first configure analog beamforming, which is formulated as a sparse signal recovery problem. Then, we propose an MMSE-based digital beamforming algorithm that iteratively minimizes the sum MSE of the user-intended data streams to reduce inter- and intra-tier interferences.

We begin by analyzing the achievable sum rate achieved by the hybrid precoders and reformulating (10) in terms of the Euclidean distance between the optimal unconstrained precoder  $\mathbf{F}_{mi}^D[k]$  and the hybrid precoders  $\mathbf{F}_i \mathbf{w}_{id_m}[k]$ . Instead of maximizing  $\sum_{i=1}^L \sum_{m=1}^{L_m} R_{mi}[k]$ , the near-optimal hybrid precoders can be obtained by minimizing  $\|\mathbf{F}_{mi}^D[k] - \mathbf{F}_i \mathbf{w}_{id_m}[k]\|_F$ . The hybrid precoder design problem can be reformulated as

$$\begin{aligned} & \arg \min_{\mathbf{W}_{mi}[k], \mathbf{F}_i, \mathbf{W}_{iu_m}[k], \mathbf{F}_{iu_m}} \sum_{i=1}^L \|\mathbf{F}_{mi}^D[k] - \mathbf{F}_i \mathbf{w}_{id_m}[k]\|_F, \\ & \text{s.t. } \text{tr}(\mathbf{W}_{mi}^*[k] \mathbf{F}_i^* \mathbf{F}_i \mathbf{W}_{mi}[k]) = P_i, \\ & \quad |\mathbf{F}_i^*(i, j)| = 1. \end{aligned} \tag{11}$$

Specifically, the method of sparse signal recovery, orthogonal matching pursuit (OMP) [22], is applied to make the hybrid precoders  $\mathbf{F}_i \mathbf{w}_{id_m}[k]$  sufficiently close to the optimal precoders  $\mathbf{F}_{mi}^D[k]$ , which is a greedy technique in which the best columns of the sensing matrix are gradually selected. In Algorithm 1, the OMP algorithm's pseudo-code is shown.  $\mathcal{F}$  is a predefined codebook and is composed of array response vectors. Using

the singular value decomposition (SVD) of the channel  $\mathbf{h}_{mi}[k] = \mathbf{U}_{mi}[k]\Sigma_{mi}\mathbf{V}_{mi}^*[k]$ , where  $\mathbf{V}_{mi}[k]$  is an  $N_i \times \text{rank}(\mathbf{h}_{mi}[k])$  unitary matrix,  $\mathbf{U}_{mi}[k]$  is an  $N_u \times \text{rank}(\mathbf{h}_{mi}[k])$  unitary matrix, and  $\Sigma_{mi} = \text{rank}(\mathbf{h}_{mi}[k]) \times \text{rank}(\mathbf{h}_{mi}[k])$  is a descending diagonal matrix of singular value. Further, two partitions of the matrices  $\Sigma_{mi}$  and  $\mathbf{V}_{mi}[k]$  are redefined as

$$\Sigma_{mi} = \begin{bmatrix} \Sigma_{mi}^1 & 0 \\ 0 & \Sigma_{mi}^2 \end{bmatrix}, \quad \mathbf{V}_{mi}[k] = [\mathbf{V}_{mi}^1[k] \quad \mathbf{V}_{mi}^2[k]], \quad (12)$$

where  $\Sigma_{mi}^1$  is an  $N_s \times N_s$  diagonal matrix and  $\mathbf{V}_{mi}^1[k]$  is an  $N_i \times N_s$  matrix. The optimal precoder  $\mathbf{F}_{mi}^D[k]$  of  $\mathbf{h}_{mi}[k]$  is defined as  $\mathbf{F}_{mi}^D[k] = \mathbf{V}_{mi}^1[k]$ , which is taken from the first  $N_s$  columns of  $\mathbf{V}_{mi}[k]$ . In summary, the beamforming algorithm selects column vectors from  $\mathcal{F}$  to form the analog precoder  $\mathbf{F}_i$ , which has a strong correlation with the residual  $\mathbf{F}_{res}[k]$ . The combiners  $\mathbf{F}_{iu_m}$  on the UEs' sides are obtained in the same manner.

---

**Algorithm 1:** Sparse beamforming via OMP.

---

**Given:**  $\mathcal{F}$  and  $\mathbf{F}_{mi}^D[k]$   
**initialization:**  $\mathbf{F}_i = \emptyset, \mathbf{F}_{res}[k] = \mathbf{F}_{mi}^D[k]$   
**1. For**  $i = 1 : L$  (for the  $i$ th BS)  
**2. For**  $l = 1 : N_i^{RF}$  (for the  $l$ th RF chain)  
**3.**  $\Psi_{il}[k] = \mathcal{F}^* \mathbf{F}_{res}[k];$   
**4.**  $e_{il} = \arg \max(\Psi_{il} \Psi_{il}^*);$   
**5.**  $\mathbf{F}_i = [\mathbf{F}_i | \mathcal{F}(:, e_{il})];$   
**6.**  $\mathbf{w}_i[k] = (\mathbf{F}_i^* \mathbf{F}_i)^{-1} \mathbf{F}_i^* \mathbf{F}_{mi}^D[k];$   
**7.**  $\mathbf{F}_{res}[k] = \frac{\mathbf{F}_{mi}^D[k] - \mathbf{F}_i \mathbf{w}_i[k]}{\|\mathbf{F}_{mi}^D[k] - \mathbf{F}_i \mathbf{w}_i[k]\|_F};$   
**8. end for**  $l$   
**9. end for**  $i$   
**10. Return**  $\mathbf{F}_i$ .

---

To manage the inter- and intra-tier interferences, the proposed MMSE-based beamforming designs find the precoders and decoders ( $\mathbf{W}_{mi}[k], \mathbf{W}_{iu_m}[k]$ ) to minimize the sum MSE  $\sum_{i=1}^L \sum_{m=1}^{L_m} \zeta_{mi}[k]$  of the mmWave HetNet, which is formulated as

$$\begin{aligned} & \arg \min_{\mathbf{W}_{mi}[k], \mathbf{W}_{iu_m}[k]} \sum_{i=1}^L \sum_{m=1}^{L_m} \zeta_{mi}[k], \\ & \text{s.t. } \text{tr}(\mathbf{W}_{mi}^*[k] \mathbf{F}_i^* \mathbf{F}_i \mathbf{W}_{mi}[k]) = P_i. \end{aligned} \quad (13)$$

The MSE  $\zeta_{mi}[k]$  of the  $m$ th UE in the  $i$ th cell is defined as

$$\zeta_{mi}[k] = \text{tr}((\bar{\mathbf{y}}_{mi}[k] - \mathbf{s}_i[k])(\bar{\mathbf{y}}_{mi}[k] - \mathbf{s}_i[k])^*), \quad (14)$$

where  $\bar{\mathbf{y}}_{mi}[k]$  is the effective received signal matrix, which is expressed as

$$\bar{\mathbf{y}}_{mi}[k] = \mathbf{W}_{iu_m}[k] \bar{\mathbf{H}}_{mi}[k] \mathbf{W}_{mi}[k] \mathbf{s}_i[k] + \sum_{j \neq i}^L \mathbf{W}_{iu_m}[k] \bar{\mathbf{H}}_{mi}[k] \mathbf{W}_{mj}[k] \mathbf{s}_j[k] + \mathbf{W}_{iu_m}[k] \mathbf{n}_i[k]. \quad (15)$$

Here, we denote  $\bar{\mathbf{H}}_{mi}[k] = \mathbf{F}_{iu_m} \mathbf{H}_{mi}[k] \mathbf{F}_i$  as the effective channel and  $\bar{\mathbf{n}}_i[k] = \mathbf{W}_{iu_m}[k] \mathbf{n}_i[k]$  as the effective noise. After several mathematical manipulations, (14) can be written as

$$\begin{aligned} \zeta_{mi}[k] &= \text{tr}(\Phi_{si}[k] - \mathbf{W}_{iu_m}[k] \bar{\mathbf{H}}_{mi}[k] \mathbf{W}_{mi}[k] \Phi_{si}[k] - \Phi_{si}[k] \mathbf{W}_{mi}^*[k] \bar{\mathbf{H}}_{mi}^*[k] \mathbf{W}_{iu_m}^*[k]) \\ &+ \text{tr}(\mathbf{W}_{iu_m}[k] (\bar{\mathbf{H}}_{mi}[k] (\sum_{j \in D} \mathbf{W}_{mj}[k] \Phi_{sj}[k] \mathbf{W}_{mj}^*[k]) \bar{\mathbf{H}}_{mi}^*[k] + \Phi_{ni}[k]) \mathbf{W}_{iu_m}^*[k]), \end{aligned} \quad (16)$$

where  $\Phi_{si}[k] = \mathbf{s}_i[k]\mathbf{s}_i^*[k]$  is denoted as the source covariance matrix.  $\Phi_{ni}[k] = \bar{\mathbf{n}}_i[k]\bar{\mathbf{n}}_i^*[k]$  and  $D = \{1, \dots, L\}$ . For the with-cooperation case,  $\Phi_{ni}[k] = \bar{\mathbf{n}}_i[k]\bar{\mathbf{n}}_i^*[k] + \bar{\mathbf{H}}_{mi}[k](\sum_{j \neq i}^L \mathbf{W}_{mj}[k]\Phi_{sj}[k]\mathbf{W}_{mj}^*[k])\bar{\mathbf{H}}_{mi}^*[k]$  and  $D = \{j\}$  for the without-cooperation case. Setting  $\zeta_{mi}[k]$ 's gradient to zero with respect to  $\mathbf{W}_{iu_m}[k]$ , for the given  $\mathbf{W}_{mi}[k]$ , the MMSE decoder can be defined as

$$\mathbf{W}_{iu_m}[k] = \frac{\Phi_{si}[k]\mathbf{W}_{mi}^*[k]\bar{\mathbf{H}}_{mi}^*[k]}{\bar{\mathbf{H}}_{mi}[k](\sum_{j \in D} \mathbf{W}_{mj}[k]\Phi_{sj}[k]\mathbf{W}_{mj}^*[k])\bar{\mathbf{H}}_{mi}^*[k] + \Phi_{ni}[k]}. \tag{17}$$

Instead of using (14), the Lagrange multipliers approach can be used to formulate an augmented cost function for addressing the problem (13). The alternative augmented cost function can be expressed as

$$\eta_{mi}[k] = \zeta_{mi}[k] + \text{tr}(\Lambda(\mathbf{W}_{mi}^*[k]\mathbf{F}_i^*\mathbf{F}_i\mathbf{W}_{mi}[k] - P_i)), \tag{18}$$

where  $\Lambda_m = \text{diag}(\lambda_{m1} \dots \lambda_{mL})$ , and  $\lambda_{mi}$  is the Lagrange multiplier. For the given  $\mathbf{W}_{iu_m}[k]$ , setting the gradient of  $\eta_{mi}[k]$  to zero with respect to  $\mathbf{W}_{mi}[k]$ , the MMSE precoder can be obtained as

$$\mathbf{W}_{mi}[k] = \frac{\bar{\mathbf{H}}_{mi}^*[k]\mathbf{W}_{iu_m}^*[k]}{\sum_{j \in D} \bar{\mathbf{H}}_{mj}^*[k]\mathbf{W}_{ju_m}^*[k]\mathbf{W}_{ju_m}[k]\bar{\mathbf{H}}_{mi}[k] + \Lambda_m}. \tag{19}$$

We set the gradient of  $\eta_{mi}[k]$  to zero with respect to  $\mathbf{W}_{mi}[k]$ , the Lagrange multiplier is defined as

$$\begin{aligned} \lambda_{mi} = \text{tr}(\sum_{i \in D} \mathbf{W}_{mi}[k]\Phi_{si}^2[k]\mathbf{W}_{mi}^*[k]\bar{\mathbf{H}}_{mi}^*[k]\mathbf{B}_{mi}[k]\bar{\mathbf{H}}_{mi}[k] - (\mathbf{W}_{mi}^*[k]\mathbf{F}_i^*\mathbf{F}_i\mathbf{W}_{mi}[k]) \\ \sum_{j \in D} \bar{\mathbf{H}}_{mj}^*[k]\mathbf{B}_{mj}[k]\bar{\mathbf{H}}_{mj}[k]\mathbf{W}_{mj}[k]\Phi_{sj}^2[k]\mathbf{W}_{mj}^*[k]\bar{\mathbf{H}}_{mj}^*[k]\mathbf{B}_{mj}[k]\bar{\mathbf{H}}_{mj}[k])P_i^{-1}, \end{aligned} \tag{20}$$

where  $\mathbf{B}_{mj}[k] = (\bar{\mathbf{H}}_{mi}[k](\sum_{j \in D} \mathbf{W}_{mj}[k]\Phi_{sj}[k]\mathbf{W}_{mj}^*[k])\bar{\mathbf{H}}_{mi}^*[k] + \Phi_{ni}[k])^{-1}$ . The procedures of the proposed MMSE-based iterative algorithm jointly finding the sub-optimum precoders and decoders is generalized in Algorithm 2. The formulas in (17), (19) and (20) are calculated iteratively until the stop criteria are satisfied to yield the MMSE precoders and decoders. We define the termination criterion as follows to ensure the viability of the initial constraint problem:

$$|M^{(n)} - M^{(n-1)}| \leq \epsilon, \tag{21}$$

where  $\epsilon$  is a minor tolerance that impacts the algorithm's precision and  $M^{(n)}$  represents the objective value of (18) in the iteration  $n$ .

---

**Algorithm 2:** The proposed generalized iterative algorithm.

---

**Initialize:**  $\mathbf{W}_{mi}[k]$ ,  $\mathbf{W}_{iu_m}[k]$  and  $\Lambda$  with random values

1. set  $n = 0$ ;
  2. **while**  $|M^{(n)} - M^{(n-1)}| > \epsilon$  or  $n < N_{\max}$  **do**
  3. For given  $\mathbf{W}_{mi}^{(n-1)}[k]$ , update  $\mathbf{W}_{iu_m}^{(n)}[k]$  by (16);
  4. For given  $\mathbf{W}_{iu_m}^{(n-1)}[k]$ , update  $\Lambda_m$  or  $\lambda_{mi}$  by (19);
  5. For given  $\mathbf{W}_{iu_m}^{(n)}[k]$  and  $\Lambda$ , update  $\mathbf{W}_{mi}^{(n)}[k]$  by (18);
  6. Calculate  $M^{(n)}$  via (20);
  7. Let  $n = n + 1$ ;
  8. **end while**
  9. **Return**  $\mathbf{W}_{mi}[k]$ ,  $\mathbf{W}_{iu_m}[k]$ , and  $\Lambda_m$ .
-

Interference alignment (IA) is another approach to mitigating the inter- and intra-tier interferences. The main idea of IA is to align the interference from the transmitters to the reduced-dimensional subspace of the receivers. As shown in Figure 1, the following conditions should be satisfied to achieve IA:

$$\mathbf{W}_{ju_m}[k]\mathbf{h}_{mj}[k]\mathbf{w}_{id_m}[k] = \mathbf{0}, j \neq i, 1 \leq j, i \leq L_1 \quad (22)$$

$$\mathbf{W}_{ju_m}[k]\mathbf{h}_{m1}[k]\mathbf{w}_{1d_m}[k] = \mathbf{0}, L_1 + 1 \leq j, i \leq L \quad (23)$$

$$\mathbf{W}_{1u_m}[k]\mathbf{h}_{mi}[k]\mathbf{w}_{id_m}[k] = \mathbf{0}, L_1 + 1 \leq j, i \leq L \quad (24)$$

$$\text{rank}(\mathbf{W}_{ju_m}[k]\mathbf{h}_{mj}[k]\mathbf{w}_{id_m}[k]) = N_s, 1 \leq j, i \leq L \quad (25)$$

where  $L_1$  is the number of BSs in sub-system 1. The inter-cell interference among the picocells and the interference between the picocells and macrocell in sub-system 1 are mitigated via (22). Equation (23) addresses the interference from the MBS to PUs in sub-system 2. Equation (24) mitigates the interference from the picocell base stations (PBSs) in sub-system 2 to the MUs. Equation (25) guarantees that the signal space is orthogonal to the corresponding interference subspace and has  $N_s$  dimensions.

## 6. Simulation Results

The performance of the proposed hybrid beamforming designs for the two-tier multi-user downlink mmWave HetNet was evaluated. The mmWave HetNet comprises one macrocell and nine picocells. The radii of the macrocell and picocells are 500 m and 40 m, respectively. The MBS, PBSs, and UEs' sides are equipped with  $N_m = 144$ ,  $N_p = 64$ , and  $N_u = 36$  antennas, respectively. The central carrier frequency is 28 GHz with an 850 MHz bandwidth.  $K = 128$  is the number of subcarriers. The environment for propagation has  $C = 5$  clusters and  $R_c = 20$  rays per cluster. The delay spread of each cluster is determined to be  $\tau_c = 2.7$  ns. The relative time delay for each ray results from the zero-mean normal distributions with  $\tau_{r_c} = 0.27$  ns. The mean AoAs/AoDs for each cluster are calculated using  $[-\frac{\pi}{3}, \frac{\pi}{3}]$ . The relative AoA/AoD shifts are derived from a Gaussian distribution with  $\{\vartheta_{r_c}, \varphi_{r_c}\} = 2^\circ$ . A raised cosine filter is utilized as the pulse-shaping filter with a factor of 1. The transmit power is set at 64dBm in the macrocell and 15dBm in the picocells. The achievable sum rate as the optimal objective is used for the performance comparison of the hybrid beamforming designs of multi-user mmWave HetNets, which is defined as

$$R = \frac{1}{K} \sum_{m=1}^{L_m} \sum_{k=1}^K \sum_{i=1}^L \log_2 \left( 1 + \frac{P_i \|\mathbf{W}_{iu_m}^*[k]\mathbf{F}_{iu_m}^* \mathbf{H}_{mi}[k]\mathbf{F}_i \mathbf{W}_{mi}[k]\|_F}{K\sigma_i^2 \|\mathbf{W}_{iu_m}[k]\|_F} \right). \quad (26)$$

In this section, we compare the performance of the proposed hybrid beamforming designs in the with-cooperation scenario (HBF with cooperation) and the without-cooperation scenario (HBF without cooperation) to the optimal beamforming (optimal BF) designs and interference alignment (IA)-based hybrid beamforming (HBF IA) schemes under different cellular cooperation and data transmission scenarios. The benchmark is the performance of the optimal beamforming designs in which streams are sent along the channel's dominant eigenmodes. Figure 3 shows the spectral efficiencies of the proposed hybrid beamforming algorithms and other hybrid beamforming schemes under different effective transmit SNRs. The number of RF chains is set as 6 for the MBS and 3 for PBSs, with the number of data streams set as  $N_s = 2$  or 3. The spectral efficiencies of the proposed MMSE-based hybrid beamforming schemes are essentially close to those achieved by the optimal beamforming solution in the case of  $N_s = 3$ , as shown in Figure 3. The achievable sum rate of the HBF with-cooperation algorithms is higher than those of the HBF without-cooperation algorithms and IA-based hybrid beamforming algorithms. The performance gap among the proposed MMSE-based HBF with-cooperation, HBF without-cooperation, and IA-based hybrid beamforming algorithms increase with the increasing SNR. It turns out that compared to the IA-based or MMSE-based without-cooperation algorithms, the proposed MMSE-based with-cooperation algorithms are more able to reduce interference. As a result, in

the with-cooperation scenario, the entire HetNet transforms into a big single-user MIMO system and inter-cell interference no longer exists; only inter-data-stream interference has to be addressed. When comparing the results of the proposed MMSE-based hybrid beamforming algorithms to those of the optimal beamforming framework and IA-based hybrid beamforming schemes with different data transmission scenarios, the larger data stream schemes yield a better achievable sum rate. Because of the larger data stream transmission schemes leveraging the additional degrees of freedom offered by the MIMO mmWave HetNet, the proposed MMSE-based with-cooperation algorithms yield a better achievable sum rate than the MMSE-based without-cooperation algorithms and IA-based hybrid beamforming schemes.

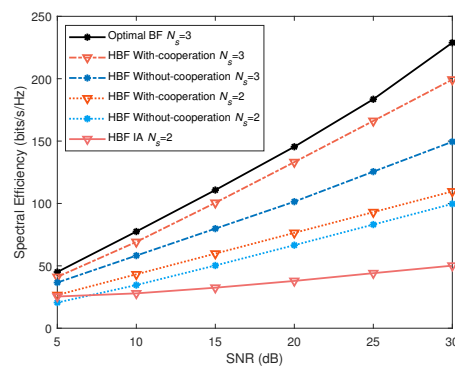


**Figure 3.** Effective system sum rate versus SNR.

Figures 4 and 5 show the achievable sum rates of the hybrid beamforming designs with different numbers of UEs in the mmWave HetNet for different SNRs. As illustrated in Figure 4, with the number of pUEs  $L_i$  in the  $i$ th picocell increasing, the performance attained by the hybrid beamforming algorithms greatly improves. The data stream is configured with  $N_s = 1$  and the number of pUEs in each picocell is configured with  $L_i = 2$  or 3. The spectral efficiencies of the proposed MMSE-based hybrid beamforming strategies are similar to those of the optimal beamforming designs. The proposed MMSE-based hybrid beamforming with-cooperation schemes outperform the without-cooperation schemes, as the with-cooperation hybrid beamforming designs are noise limited, whereas the without-cooperation hybrid beamforming schemes are interference limited. The IA-based hybrid beamforming designs cannot outperform the MMSE-based hybrid beamforming designs with an increasing SNR. The difference in performance between the proposed MMSE-based hybrid beamforming approach and the IA-based hybrid beamforming designs becomes greater with an increasing number of pUEs. In Figure 5, the performance of the proposed hybrid beamforming designs is improved with an increasing number of macrocell UEs (mUEs). This performance is achieved with the number of data streams set as  $N_s = 1$  or 2. The increase in the data streams has a significant impact on the improvement of the spectral efficiencies of the proposed MMSE-based hybrid beamforming schemes. The achievable system sum rates of the MMSE-based hybrid beamforming strategies considerably outperform those of the IA-based hybrid beamforming solutions. The proposed MMSE-based hybrid beamforming algorithms perform nearly as well as the optimal beamforming designs. It turns out that the proposed hybrid beamforming strategies are quite efficient for managing the inter- and intra-tier interferences in the mmWave HetNets.

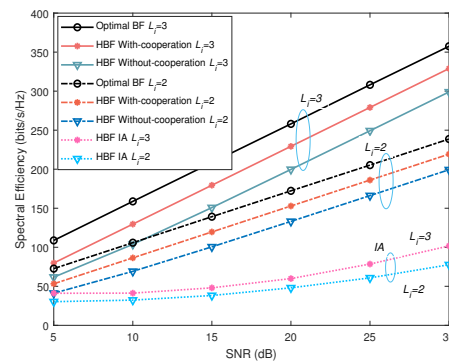


Figure 4. Effective system sum rate versus SNR.

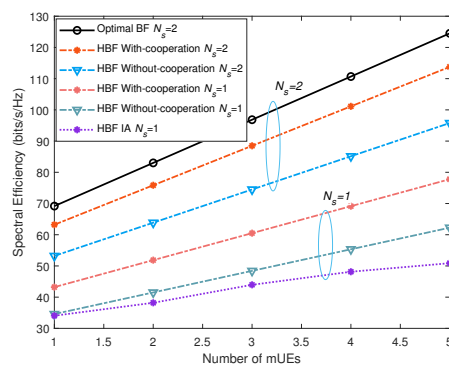


Figure 5. Effective system sum rate versus the number of mUEs.

## 7. Conclusions

In this paper, we proposed an MMSE-based hybrid beamforming strategy for downlink MIMO two-tier mmWave HetNets. First, the analog beamforming algorithm was generalized by the orthogonal matching pursuit technique and the optimization problem was formulated as the sparse signal recovery problem. Then, an MMSE-based digital beamforming strategy was proposed to minimize the sum MSE of the user-intended data streams that iteratively mitigates both the inter- and intra-tier interferences. The simulation results demonstrate that the proposed hybrid beamforming designs achieve superior performance under different cellular cooperation and data transmission scenarios.

**Author Contributions:** Conceptualization, Z.L.; methodology, Z.L.; software, Z.L.; validation, Z.L.; formal analysis, Z.L.; investigation, Z.L.; resources, Z.L.; data curation, Z.L.; writing—original draft preparation, Z.L.; writing—review and editing, Z.L.; visualization, T.C.; supervision, T.C.; project administration, T.C.; funding acquisition, T.C. All authors have read and agreed to the published version of the manuscript.

**Funding:** This work is partially supported by the National Natural Science Foundation of China (No. 62071137) and the Fundamental Research Funds for the Central Universities (No. 3072022CF0802).

**Conflicts of Interest:** The authors declare no conflict of interest. The funders had no role in the design of the study; in the collection, analyses, or interpretation of data; in the writing of the manuscript; or in the decision to publish the results.

## References

1. Heath, R.W.; lez-Prelcic, N.G.; Rangan, S.; Roh, W.; Sayeed, A.M. An Overview of Signal Processing Techniques for Millimeter Wave MIMO Systems. *IEEE J. Sel. Topics Signal. Process.* **2016**, *10*, 436–453. [[CrossRef](#)]
2. Alkhateeb, A.; Mo, J.; les-Prelcic, N.G.; Heath, R.W., Jr. MIMO precoding and combining solutions for millimeter-wave systems. *IEEE Commun. Mag.* **2014**, *52*, 122–131. [[CrossRef](#)]
3. Swindlehurst, A.; Ayanoglu, E.; Heydari, P.; Capolino, F. Millimeter-wave massive MIMO: The next wireless revolution? *IEEE Commun. Mag.* **2014**, *52*, 52–62.

4. Ali, A.; Iez-Prelcic, N.G.; Heath, R.W. Millimeter Wave Beam-Selection Using Out-of-Band Spatial Information. *IEEE Trans. Wireless Commun.* **2018**, *17*, 1038–1052. [[CrossRef](#)]
5. Bogale, T.E.; Le, L.B. Massive MIMO and mmWave for 5G wireless HetNet: Potential benefits and challenges. *IEEE Veh. Technol. Mag.* **2016**, *11*, 64–75. [[CrossRef](#)]
6. Wu, W.; Yang, Q.; Gong, P.; Kwak, K.S. Energy-efficient resource optimization for OFDMA-based multi-homing heterogeneous wireless networks. *IEEE Trans. Sig. Proc.* **2016**, *64*, 5901–5913. [[CrossRef](#)]
7. Ghosh, A.; Mangalvedhe, N.; Ratasuk, R.; Mondal, B.; Cudak, M.; Visotsky, E.; Thomas, T.A.; Andrews, J.G.; Xia, P.; Jo, H.S.; et al. Heterogeneous cellular networks: From theory to practice. *IEEE Commun. Mag.* **2012**, *50*, 54–64. [[CrossRef](#)]
8. Phan, A.H.; Tuan, H.D.; Kha, H.H.; Nguyen, H.H. Beamforming optimization in multi-user amplify-and-forward wireless relay networks. *IEEE Trans. Wireless Commun.* **2012**, *11*, 1510–1520. [[CrossRef](#)]
9. Dai, L.; Wang, B.; Peng, M.; Chen, S. Hybrid precoding-based millimeter-wave massive MIMO-NOMA with simultaneous wireless information and power transfer. *IEEE J. Sel. Areas Commun.* **2019**, *37*, 131–141. [[CrossRef](#)]
10. Alkhateeb, A.; Leus, G.; Heath, R.W., Jr. Limited feedback hybrid precoding for multi-user millimeter wave systems. *IEEE Trans. Wireless Commun.* **2015**, *14*, 6481–6494. [[CrossRef](#)]
11. Huang, H.; Song, Y.; Yang, J.; Gui, G.; Adachi, F. Deep-Learning-Based Millimeter-Wave Massive MIMO for Hybrid Precoding. *IEEE Trans. Veh. Tech.* **2019**, *68*, 3027–3032. [[CrossRef](#)]
12. Li, Z.; Zhang, C.; Lu, L.; Jia, X. Hybrid Precoding Using Out-of-Band Spatial Information for Multi-User Multi-RF-Chain Millimeter Wave Systems. *IEEE Access* **2020**, *8*, 50872–50883. [[CrossRef](#)]
13. Wang, Z.; Li, M.; Tian, X.; Liu, Q. Iterative Hybrid Precoder and Combiner Design for mmWave Multiuser MIMO Systems. *IEEE Commun. Lett.* **2017**, *21*, 1581–1584. [[CrossRef](#)]
14. Magueta, R.; Castanheira, D.; Silva, A.; Dinis, R.; Gameiro, A. Hybrid Iterative Space-Time Equalization for Multi-User mmW Massive MIMO Systems. *IEEE Trans. Commun.* **2017**, *65*, 608–620. [[CrossRef](#)]
15. Satyanarayana, K.; El-Hajjar, M.; Kuo, P.H.; Mourad, A.; Hanzo, L. Hybrid beamforming design for full-duplex millimeter wave communication. *IEEE Trans. Veh. Technol.* **2019**, *68*, 1394–1404. [[CrossRef](#)]
16. Castanheira, D.; Lopes, P.; Silva, A.; Gameiro, A. Hybrid Beamforming Designs for Massive MIMO Millimeter-Wave Heterogeneous Systems. *IEEE Access* **2017**, *5*, 21806–21817. [[CrossRef](#)]
17. Li, Z.; Chen, T.; Hu, X. Hybrid beamforming for millimeter-wave massive MIMO heterogeneous networks. *Digit. Signal Process.* **2022**, *130*, 103738. [[CrossRef](#)]
18. Wang, X.; Gursoy, M.C. Coverage analysis for energy-harvesting UAV-assisted mmWave cellular networks. *IEEE J. Sel. Areas Commun.* **2019**, *37*, 2832–2850. [[CrossRef](#)]
19. Turgut, E.; Gursoy, M.C. Coverage in Heterogeneous Downlink Millimeter Wave Cellular Networks. *IEEE Trans. Commun.* **2017**, *65*, 4463–4477. [[CrossRef](#)]
20. Maso, M.; Debbah, M.; Vangelista, L. A distributed approach to interference alignment in ofdm-based two-tiered networks. *IEEE Trans. Veh. Technol.* **2013**, *62*, 1935–1949. [[CrossRef](#)]
21. Sharma, S.; Chatzinotas, S.; Ottersten, B. Interference alignment for spectral coexistence of heterogeneous networks. *EURASIP J. Wireless Commun. Netw.* **2013**, *2013*, 46. [[CrossRef](#)]
22. Ayach, O.E.; Rajagopal, S.; Abu-Surra, S.; Pi, Z.; Heath, R.W. Spatially Sparse Precoding in Millimeter Wave MIMO Systems. *IEEE Trans. Wireless Commun.* **2014**, *13*, 1499–1513. [[CrossRef](#)]